One Step Dimethyl Ether (DME) Synthesis from CO2 Hydrogenation over Hybrid Catalysts Containing Cu/ZnO/Al2O3 and Nano-Sized Hollow ZSM-5 Zeolites

Karima Krim, Alexander Sachse, Anthony Le Valant, Yannick Pouilloux, Smain Hocine

One Step Dimethyl Ether (DME) Synthesis from CO_2 Hydrogenation over Hybrid Catalysts Containing Cu/ZnO/Al_2O_3 and Nano-Sized Hollow ZSM-5 Zeolites

Karima Krim[1] · Alexander Sachse[2] · Anthony Le Valant[2] · Yannick Pouilloux[2] · Smain Hocine[1]

Abstract

The study has focused on the development of bifunctional catalytic materials for the direct DME synthesis from CO_2/H_2. The industrial Cu/ZnO/Al_2O_3 is used as the copper based catalyst for the first step of the methanol synthesis from CO_2/H_2. It will be combined with hollow nano-ZSM-5 zeolites with mesoporous shell as the acid catalyst of the second step the methanol dehydration to DME. The bifunctional materials will be tested in the direct DME synthesis from CO_2/H_2 under the following conditions: $T = 225$ °C, $p = 30$ bar, $H_2/CO_2 = 3$. Under our reaction conditions, CO was not observed, only the DME majority product (77.5%) and CH_3OH (22.5%) were obtained.

Graphical Abstract

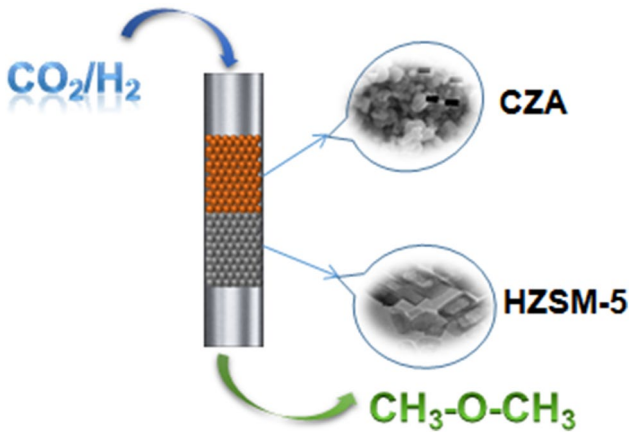

Keywords DME synthesis · CO_2 hydrogenation · Nano-sized hollow ZSM-5 · Cu/ZnO/Al_2O_3

1 Introduction

Ether oxides such as dimethyl ether (DME) is considered as an alternative fuel for diesel engines and their uses include the manufacture of solvents, aerosol propellant for in deodorants, perfumes and as the feedstock for the production of the methylating agent, it is also a platform molecule for energy storage. It has long been known that CO_2 and CO can be hydrogenated, very selectively, to methanol over copper/zinc oxide based catalysts, whereas dimethyl ether is

✉ Smain Hocine
smain.hocine@ummto.dz

[1] Laboratoire de Chimie Appliquée Et de Génie Chimique, Université M. Mammeri de Tizi-Ouzou, BP. 17 R.P 1500, Tizi-Ouzou, Algeria

[2] Institut de Chimie Des Milieux Et Matériaux de Poitiers (IC2MP), UMR 7285, Université de Poitiers, CNRS, 4, rue Michel Brunet, 86073 Poitiers cedex 9, France

produced by dehydration of methanol over solid acid catalysts such as γ-Al_2O_3, zeolites or silica-modified alumina at temperatures ranging from 250 to 300 °C and the pressure range 10–20 bar [1–3]. The first commercial plant for the conversion of syngas to methanol was built in 1923 by BASF. The process developed by BASF is known as the high-pressure process, which operated at up to 250–350 bar and 320–450 °C, using zinc oxide/chromium-based catalyst (ZnO/Cr_2O_3) [4]. In the 1960s, Imperial Chemical Industries (ICI) developed a low-pressure process for methanol synthesis from synthesis gas (a mixture of $CO/CO_2/H_2$) using $Cu/ZnO/Al_2O_3$ catalyst operating at mild conditions 35–55 bar, 200–300 °C [5]. Today, this is the only process used to product methanol from $CO/CO_2/H_2$ mixture, according to the following reactions: [6, 7]

$$CO + 2H_2 \leftrightarrow CH_3OH \quad \Delta H^{\circ}_{298} = -91 kJ/mol \tag{1}$$

$$CO_2 + 3H_2 \leftrightarrow CH_3OH + H_2O \quad \Delta H^{\circ}_{298} = -49.4 kJ/mol \tag{2}$$

$$CO_2 + H_2 \leftrightarrow CO + H_2O \quad \Delta H^{\circ}_{298} = +41.2 kJ/mol \tag{3}$$

DME is predominantly produced commercially via the catalytic dehydration of methanol (reaction 4) over solid acid catalysts such as γ-Al_2O_3 [8, 9] and HZSM-5 zeolite [10–12].

$$2CH_3OH \leftrightarrow CH_3OCH_3 + H_2O \quad \Delta H^{\circ}_{298} = -23 kJ/mol \tag{4}$$

The direct synthesis of DME from the hydrogenation of carbon dioxide is one of the attractive approaches to utilizing CO_2 as an economical and ecological C1 source (reaction 4) [13–16].

The process of direct synthesis of DME from synthesis gas (syngas) involves (2) conversion of synthesis gas to methanol, followed by (4) dehydration of the latter to yield dimethyl ether (DME) and water, as shown below.

$$2CO_2 + 6H_2 \leftrightarrow CH_3OCH_3 + 3H_2O \quad \Delta H^{\circ}_{298} = -123 kJ/mol \tag{5}$$

Catalytic hydrogenation of CO_2 into dimethyl ether is thermodynamically favourable; however, this reaction requires the presence of a bifunctional catalyst combining a copper-based catalyst and a solid acid catalyst. It is generally admitted that HZSM-5 shows much higher activity than γ-Al_2O_3 at moderate temperature range (240–280 °C) [17, 18].

The one-pot CO_2 hydrogenation to DME involves a bifunctional catalysts exhibit metallic and acidic functions capable of performing two reactions, methanol synthesis and methanol dehydration, simultaneously. The metallic function is responsible for the hydrogenation of carbon dioxide, whereas the acidic function used for dehydration of methanol. The current research is focused on the development of a suitable catalytic system for efficient activation of carbon dioxide with selective production of DME.

The combination of Cu–Zn oxides and HZSM-5 is the basic component of the new famous hybrid catalyst, the development of which has been amply documented [17–21]. Copper zinc-HZSM-5 system display extremely high activity and produce DME with great selectivity. Other products, such as carbon monoxide, methanol and water were also obtained.

In the literature, several catalytic systems are claimed as active in the activation of carbon dioxide. The catalytic systems currently employed for the direct synthesis of DME from CO_2 are bifunctional catalysts.

The crucial issue for preparing a high-active hybrid catalyst is optimizing the composition and reaction conditions of two functional components. Li et al. [22] studied the effects of calcination temperature of the bifunctional catalysts CuO-ZnO-ZrO_2 /HZSM-5 on the physicochemical and catalytic properties for one-step synthesis of dimethyl ether (DME) from CO_2 hydrogenation and found that both the CO_2 conversion and DME selectivity of the bifunctional catalysts decrease with the increase in calcination temperature, which can be attributed to the decrease of metallic copper surface area, adsorption capacity of CO_2, specific surface area, and reducibility of CuO. Liu et al. [23] have reported that the CuO-Fe_2O_3-ZrO_2/HZSM-5 bifunctional catalyst was prepared and used for the direct synthesis of dimethyl ether (DME) from CO_2 hydrogenation. The results revealed that doping the CuO-Fe_2O_3 catalyst with ZrO_2 increase the specific surface area, CO_2 conversion and DME yield than those obtained using CuO-Fe_2O_3/HZSM-5 as catalysts.

In a very recent paper, Xin et al. [24] reported that a novel Cu–ZnO-ZrO_2/HZSM-5 catalyst developed by in situ growing HZSM-5 on Cu–ZnO-ZrO_2 nanoparticles directly via the mediated of aluminium enhanced both metal dispersion and specific surface area than the reference Cu–ZnO-ZrO_2. At the typical reaction condition of 250 °C and 5.0 MPa, the Cu–ZnO-ZrO_2/HZSM-5 exhibited remarkable catalytic performances, 34% CO_2 conversion, 67% DME selectivity, were achieved. Xinhui Zhou et al. [25] have studied a series of CuO-Fe_2O_3-CeO_2 catalysts with various CeO_2 doping mixed mechanically with HZSM-5 to perform the direct synthesis of dimethyl ether (DME) from carbon dioxide hydrogenation. The results indicated that modification of CuO-Fe_2O_3 catalyst with CeO_2 promoted the CuO dispersion, reduced the CuO crystallite size, decreased the reduction temperature of highly dispersed CuO, modified the specific surface area of the CuO-Fe_2O_3-CeO_2 catalyst, and improved the catalytic activity of the CuO-Fe_2O_3-CeO_2 catalyst. The addition of CeO_2 to CuO-Fe_2O_3 catalyst increased the amount of Lewis acid sites and Brønsted acid sites, and enhanced the acid

intensity of the weak acid sites, which in turn promoted the catalytic performance of CO_2 hydrogenation to DME. At the typical reaction condition of 260 °C and 3.0 MPa, the CO_2 conversion and DME selectivity were 20.9%, and 63.1%, respectively obtained.

In other studies, Qin et al. [26] have also reported the results of investigations of the hydrogenation of CO_2 to dimethyl ether on La, Ce-modified Cu-Fe/HZSM-5 catalysts and of the effect of catalyst composition on the CO_2 hydrogenation. The results showed that La and Ce significantly decreased the outer-shell electron density of Cu and improved the reduction ability of the Cu–Fe catalyst in comparison to the Cu-Fe-Zr catalyst, which may increase the selectivity for DME. The Cu-Fe-Ce catalyst had a greater specific surface area than the Cu-Fe-La catalyst. This promoted CuO dispersion and decreased CuO crystallite size, which increased both the DME selectivity and the CO_2 conversion. The disadvantage of Ce addition could be the formation of stable carbonates that cover the catalyst surface and thus lead to the decrease of the catalytic activity.

In 2017, Tingjun Fu et al. [27] reported that a nano-sized hollow ZSM-5 with rich mesopores in shell, prepared by the alkaline treatment method presented a large external surface area and excellent catalytic stability when used in methanol-to gasoline reaction. The external surface area was increased from 98 to 203 m^2/g, more than twice that of the untreated nano-ZSM-5. The thin shell and rich mesopores would improve its catalytic performance in many diffusion-limited reactions. The large external surface can promote the diffusion of coke precursors from micropores to external surface, reducing the generation of coke in micropores and improving the catalytic stability.

In the literature, several catalytic systems possessing acidic function are claimed as active in the dehydration of methanol, such as HZSM-5 [28, 29], SAPO-18 [30] and MCM-41 [31] MFI-type zeolites [32] and heteropolyacids [33] are also used as the acidic functions.

The hybrid catalyst, with Al_2O_3 as the acidic function, rapidly loses its catalytic activity because of the hydrophilic character. Water formed by CO_2 hydrogenation and methanol dehydration strongly adsorbs on the Lewis acid sites γ-Al_2O_3 inhibiting DME formation. This leads to blocking of the active centers on the catalyst surface, a problem that has to be overcome by high temperature [34].

Zeolites constitute another class of the catalysts of acidic character. Commonly, H-ZSM-5 is used because of its better hydrophobic character than Al_2O_3 and predominance of Brønsted-type acidity [18, 34, 35]. However, due to the high reaction temperature (≈270 °C) hydrocarbons and coke can be observed among created products. It is related to the high acidity of this zeolite. To improve its selectivity to DME and preserve high methanol conversion simultaneously, it is needed to decrease the amount of strong acid centers maintaining the total acidity at high level [29].

The purpose of this study to develop active and selective hybrid catalysts for the direct catalytic hydrogenation of CO_2 into DME at low temperature and to correlate the acid–base and metallic properties of hybrid catalysts with its catalytic activities for the carbon dioxide hydrogenation reaction.

2 Experimental

2.1 Preparation of Catalysts

2.1.1 Cu-Based Methanol Catalyst

The Cu-based methanol catalyst was a commercial sample (Alfa Aesar) in its form CuO-ZnO-Al_2O_3 denoted here as (CZA) with nominal composition (Cu:Zn:Al:Mg = 44.2:17.4:4.15:0.68 wt.%) and its particle size is 0.2–0.4 mm.

2.1.2 Zeolite Dehydration Catalysts

2.1.2.1 Synthesis of Parent Nano-ZSM-5 The parent nano-ZSM5 (denoted as ZSM5-P) was synthesized by hydrothermal method according to the procedure described in the literature [27], and using a gel with the following molar composition:

$$60SiO_2{:}1Al_2O_3{:}15TPAOH{:}500H_2O.$$

Firstly, TEOS was mixed with (TPAOH, 20 wt.%) at 80 °C and stirred for 24 h. Then, $Al(NO_3)_3$ and NaOH were dissolved in deionized water, added to the above mixture and transferred to a stainless steel Teflon lined autoclave and heated at 170 °C for 24 h. After cooling to RT a solid was recovered by centrifugation, washed with distilled water until neutral pH and dried at 50 °C overnight. Finally, the solid was calcined under an air flow at 550 °C for 8 h.

2.1.2.2 Alkaline Treatment of Parent Nano-ZSM-5 The hollow zeolite (denoted as ZSM5-H) was synthesized by treating parent nano-zeolite with NaOH solution with a liquid-to-solid ratio of 15 ml/g for 15 h at 50 °C. The solid product was washed with distilled water and dried at 50 °C overnight.

Thereafter, mesopores were introduced into the shell by a treatment with a mixed alkaline solution of (NaOH and TPAOH) for 4 h at 50 °C, with a liquid-to-solid of 15 ml/g where the total OH^- concentration in solution was 0.1 M and the molar ratio of TPAOH/(TPAOH + NaOH) was 0.25. The prepared sample was denoted as ZSM5-HM.

2.1.2.3 Microporous Zeolite

The microporous zeolite used was a commercial HZSM-5 microporous zeolite (Zeolyst Int. CBV 3024E) denoted here as ZSM5-C.

2.1.3 Hybrid CZA/Zeolite Catalysts

All the zeolites samples were pelletized, crushed and sieved until a 0.2–0.4 mm particle size. Then, the final hybrids catalysts were prepared by a physical mixture using a duel-bed arrangement, composed by a CZA methanol catalyst in first bed and a zeolite catalyst in second bed [36]. A weight ratio of CZA/zeolite used to prepare these mixture was 1/3.

The series of prepared hybrids catalysts denoted here as CZA/ZSM5-P, CZA/ZSM5-HM, CZA/ZSM5-H and CZA/ZSM5-C.

2.2 Catalysts Characterization

The elemental composition of the samples was determined by an inductively coupled plasma emission spectroscopy (ICP-OES) on an Agilent 5110 VDV.

The textural properties were determined by adsorption–desorption of nitrogen at the temperature of liquid nitrogen (− 196 °C) using a Micromeritics 3flex instrument. Surface areas (S_{BET}) were calculated by applying the Brunauer–Emmett–Teller (BET) equation. The total pore volume, the micropores volume and the external surface areas were estimated with the t-plot method. The mesopores size distribution was assessed with Barrett-Joyner-Halenda (BJH) model.

The hollow-structure with mesopores in the shell was surveyed by transmission electron microscopy (TEM) using a JEOL 2100 instrument operating at 200 kV with a LaB_6 filament, equipped with an EDAX energy dispersive spectrometer, a wide-angle annular dark field detector HAADF, and a Gatan CCD camera.

Powered X-ray diffraction patterns of synthesized samples were obtained with PANalytical Empyrean x-ray diffractometer instrument (Cu Kα radiation, λ = 1.5406, 40 kV, 30 mA, 5–50° 2θ range, scanning step 0.2°·s^{-1}).

2.3 Acidity Measurements

The in-situ FT-IR technique was used to study the surface acidity of the samples. FTIR measurements were carried out on a Nicolet 5700-FTIR spectrometer with an optical resolution of 2 cm^{-1}, using pyridine as a molecular probe [37].

Total acidity and acid strength distribution both of zeolites and hybrid catalysts was determined by temperature programmed desorption of ammonia (NH_3-TPD). The samples were placed in a micro-reactor (U-type) connected to a thermal conductivity detector (TCD) and pre-treated at 400 °C under H_2 for 1 h, then cooled to 100 °C. Afterwards, the samples were saturated with ammonia (5vol.% in He) for 30 min. After the treatment in flow of He to remove the physisorption NH_3, the NH_3 chemisorbed was evacuated over the temperature range of 100–750 °C at rate of 2 °C/m under He.

2.4 Catalytic Tests

The catalytic hydrogenation of CO_2 to DME was carried out in a high-pressure stainless-steel fixed-bed tubular reactor by feeding a reaction mixture of H_2 and CO_2 in the molar ratio of $CO_2/H_2 = 1:3$. Prior to the activity measurements, the samples were reduced in situ at 400 °C (at a heating rate of 5 °C/min) under a flow of pure hydrogen (30 ml/min) at atmospheric pressure for 30 min. The reaction was performed at 30 bar overall pressure and with a GHSV = 48,000 NL/h/kg_{cat}. Catalytic activity was measured between 200 and 350 °C for 5 h. The effluents from the reactor were analysed using a Agilent 7890 A gas chromatograph connected online to the reactor, equipped with two channels: The first channel consisted of two series-connected of HP PLOT 5A molecular sieve column for (H_2 and CO) and an HP PLOT Q molecular sieve column for (CO_2 and H_2O) connected to a TCD detector, while the second channel consisted of an HP INNOWAX capillary column (for methanol and dimethyl ether) connected to a FID detector. All analysis lines and valves connecting the reactor with the GC were heated at 250 °C to avoid a possible condensation of the products before entering the gas chromatograph.

3 Results and Discussion

3.1 Textural, Structural and Chemical Proprieties

Textural properties of different zeolites were determined by N_2 physisorption at 77 K. The isotherms of ZSM5-C and ZSM5-P present Type I shape, which is typical of for microporous materials [38]. The increase in nitrogen uptake at high relative pressure is due to the intercrystalline adsorption, typical for nano-zeolites (Fig. 1a).

After alkaline treatment of ZSM5-P with NaOH and NaOH/TPAOH solution, the ZSM5-H and ZSM5-HM exhibit a higher equivalent BET surface area compared to the parent zeolite (ZSM5-P), indicating the formation of mesoporosity. Upon alkaline treatment the isotherms feature a type 4 hysteresis loop, which is due to cavitation, typical for occulted mesopores arising from alkaline treatment [39]. Mesopore volume increases as a result of alkaline treatment, indicating the hierarchization of the parent sample. ZSM5-HM features the highest mesopore volume, i.e. 0.25 cm^3/g,

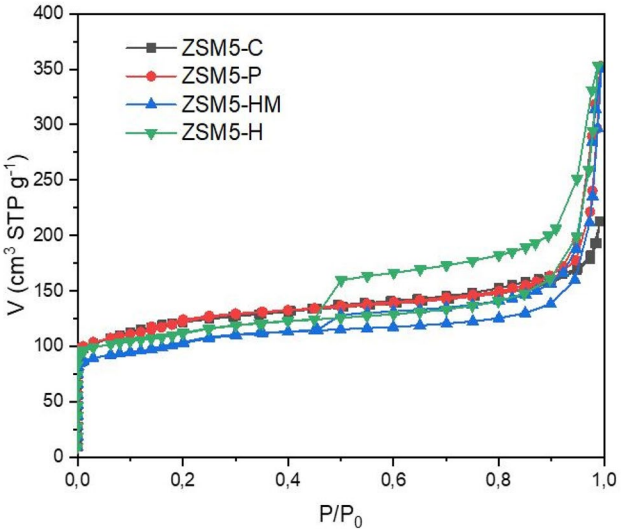

Fig. 1 Nitrogen physisorption isotherms at 77 K

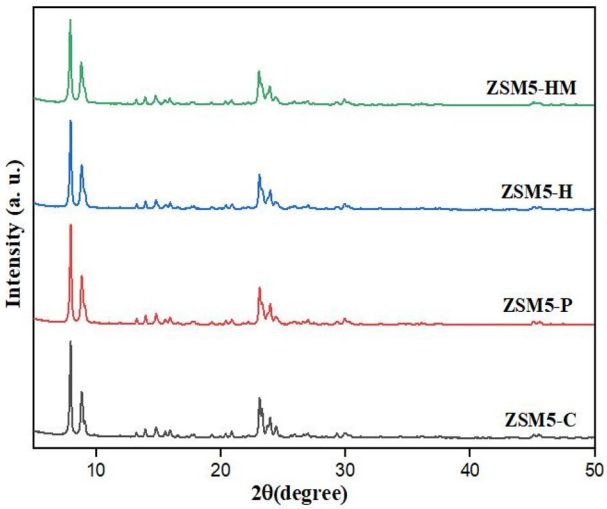

Fig. 2 X-ray diffraction patterns of the samples

whilst presenting equivalent micropore volume as the parent sample (ZSM5-P) (Table 1). The larger mesopore volume obtained for CZA/ZSM5-HM is due to their small crystal size and the corresponding intercrystalline porosity.

The increase in the external surface area for the hierarchical samples further indicates the development of secondary porosity.

From the XRD patterns, all the characteristic peaks for the MFI structure can be observed in all samples (Fig. 2) [40]. The absence of a large peak centred at 20–25 degrees 2θ indicates that no amorphization occurred during the alkaline treatments. Relative crystallinity decreases slightly for the hierarchical ZSM-5 samples, which can be ascribed to the development of secondary porosity upon alkaline treatment.

Further insight on the textural properties was obtained by comparing the TEM images of the parent and of the hierarchical samples (Fig. 3a). The parent zeolite (ZSM-5P) presents typical crystal morphology of the MFI phase, with crystal sizes comprised of 50–100 nm. Upon alkaline treatment with NaOH (ZSM5-H) a large electron clear area can be distinguished at within the zeolite crystals, indicating the formation of nano-boxes (Fig. 3b). ZSM5-HM allows for distinguishing additional mesoporosity within the shell of the nano-boxes (Fig. 3c).

Temperature-programmed desorption of ammonia (NH_3-TPD) [41] and Fourier transform infrared spectroscopies of pyridine adsorption [42] were employed to characterize acid properties of different samples. As shown in Fig. 4a and b, there were two NH_3 desorption peaks. The first peak at a relatively lower temperature was attributed to weak acid sites, and the second peak at a relatively higher temperature belonged to strong acid sites.

As shown in Fig. 5, in situ pyridine FTIR spectrum indicates that the peak at about 1540 cm^{-1} corresponds to pyridine adsorbed on the Brønsted acid sites, while the peak near 1450 cm^{-1} is ascribed to pyridine adsorbed on Lewis acid

Table 1 Textural properties of parent and desilicated ZSM-5 zeolites

Samples	Crystallinity (%)[a]	Crystal size (nm)	Si/Al[b]	S_{ext}[c] (m^2/g)	V_{micro}[d] (cm^3/g)	V_{meso}[e] (cm^3/g)
ZSM5-C	100	185.4	34	61	0.17	0.10
ZSM5-P	100	85.1	37	68	0.17	0.18
ZSM5-H	92	88.5	32	54	0.15	0.17
ZSM5-HM	89	92	28	72	0.15	0.25

[a]The relative crystallinity is calculated by the equation: (peak intensity of discussed sample)/(peak intensity of ZSM5-C) × 100%

[b]Determined by ICP-OES

[c]Derived the t-plot

[d]Calculated by t-plot method

[e]Calculated by total pore volume minus micropore volume

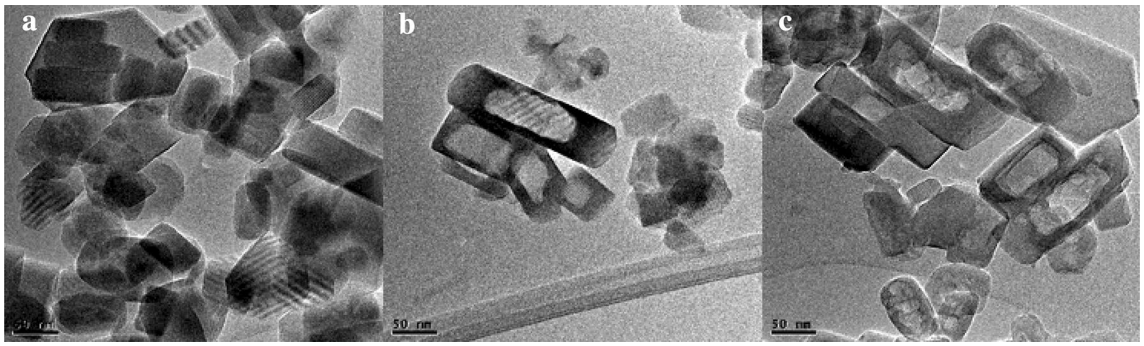

Fig. 3 TEM micrographs of ZSM5-P (**a**), ZSM5-H (**b**) and ZSM5-HM (**c**)

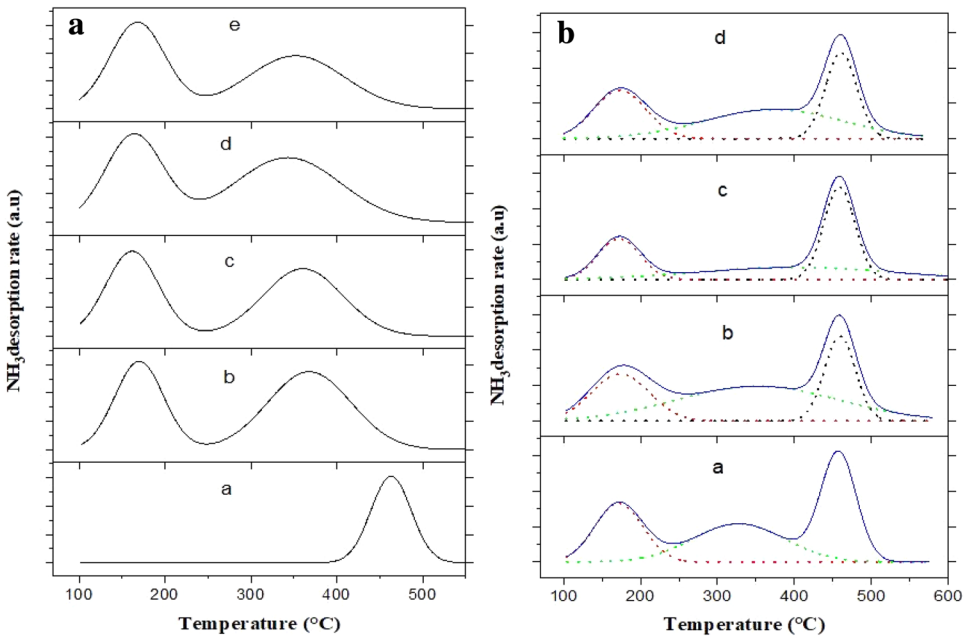

Fig. 4 **a** NH_3 desorption profiles: **a** CZA; **b** ZSM5-C; **c** ZSM5-P; **d** ZSM5-H and **e** ZSM5-HM; **4b** NH_3 desorption profiles: **a** CZA/ZSM5-C; **b** CZA/ZSM5-P; **c** CZA/ZSM5-H and **d** CZA/ZSM5-HM

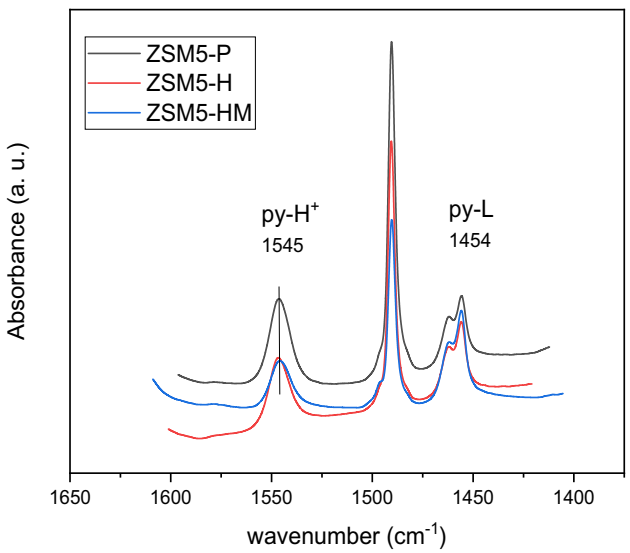

Fig. 5 FTIR spectra of adsorbed pyridine of samples

sites; the band around 1490 cm^{-1} is due to the vibrations of the H-bonded pyridine that involves the above two types of acid sites, and this band is characteristic of the total acidity of the material [43].

Table 2 lists the acidic properties of all the compounds studied by IR spectroscopy of pyridine adsorbed and Temperature-programmed desorption of ammonia (NH_3-TPD).

The results obtained IR spectroscopy of pyridine, adsorption show that the alkaline treatment of the parent zeolite improves the Brønsted acidity, while the Lewis acidity decreases after the alkaline treatment with NaOH caused by the decrease of Si/Al. The best Lewis and Brønsted acidity is observed on the zeolite treated with the NaOH/TBAOH solution (ZSM5-HM) [44], which has developed mesopores responsible for the formation of new acid sites.

From Table 2, it can be seen that the methanol synthesis catalyst (CZA) exhibits strong acid sites corresponding to ammonia desorbed at high temperature from strongly acidic

Table 2 The acidic properties of different samples

Samples	Distribution of acid sites[a] (μmol/g)				Acidity[b] (μmol/g)	
	Total	Weak	Moderate	Strong	Bronsted	Lewis
CZA	415	–	–	415.0	–	–
ZSM5-C	521	207.3	313.7	–	302	36
ZSM5-P	305	139.1	165.9	–	217	36
ZSM5-H	249	107.2	141.8	–	221	29
ZSM5-HM	468	225.6	242.4	–	276	43
CZA/ZSM5-C	616	174.2	221.2	220.6	–	–
CZA/ZSM5-P	807	199.7	414.2	193.3	–	–
CZA/ZSM5-H	511	125.3	174.1	211.6	–	–
CZA/ZSM5-HM	711	195.4	312.6	209.0	–	–

[a]Determined by NH3-TPD

[b]Determined by Py-IR

sites [46] with a desorption quantity of 0.41 mmol/g. On the other hand, zeolites display two types of acid sites, the weak acid sites, corresponding to the desorption of weakly bound ammonia. This acidity has a considerable influence on the mobility of protons in the zeolite [46, 47]; and the average acid sites corresponding to the desorbed ammonia of the Brønsted acid sites of the silanol, Al(OH)Si groups and the extra-framework aluminium species [19, 48].

The hybrid CZA/ZSM5 catalysts displayed a very high total acidity with an average acid site population of 50% is obtained on CZA/ZSM5-P. A small increase in acidity is observed for CZA/ZSM5-P compared to ZSM5-C alone, this can be explained by the high external surface of the standard zeolite which of 68 m^2/g against 61 m^2/g for the ZSM5-P. A large external surface area of the zeolite increases the interaction and exchange of Cu^{2+} ions of CZA with the hydroxyl groups of zeolites.

The order of conversion of methanol is Nano-ZSM-5 > Meso-ZSM-5 > > Con-ZSM-5, which is the same order as surface area and the reverse order of crystal size.

3.2 Effect of Temperature

The effects of temperature on the CO_2 conversion and the products distribution were examined in the temperature range of 200–350 °C at 30 bar and $H_2/CO_2 = 3$, over CZA/ZSM5 catalysts with a weight ratio CZA/ZSM5 = 0.5. In our reaction conditions, the hydrogenation of CO_2 mainly produced methanol and dimethyl ether, but the formation of CO took place simultaneously through the RWGS side reaction.

With increasing the reaction temperature, the conversion of CO_2 increases from 1.15 up to 16.58%, but the selectivity of CH_3OH and DME decreased from 44.3 to 2.5% and from 54.2 to 0.5%, when the reaction temperature was increased from 200 to 350 °C (Table 3). CO formation is favoured at a high-temperature, which reduces CH_3OH and DME selectivity drastically. This is probably because the reverse water–gas shift reaction is favourable in thermodynamics at higher reaction temperatures, so CO production becomes dominant at high reaction temperatures.

Table 3 Effects of temperature on the conversion of CO_2 and the product selectivity of CZA/ZSM5-C ($p = 3$ MPa, $H_2/CO_2 = 3$)

T (°C)	X_{CO_2}(%)	S_{MeOH} (%)	S_{CO} (%)	S_{DME} (%)
200	1.15	44.3	0.0	54.2
250	8.70	20.4	53.3	26.1
300	17.17	9.1	83.3	7.4
350	16.58	2.5	96.7	0.5

From Table 3, we can see a high temperature, enhances the conversion to CO_2, but the disadvantage is that the CO is produced at the same time as the methanol and dimethyl ether.

The best catalytic performance in terms of oxygenated products (CH_3OH and DME) selectivity was obtained between 200 and 250 °C at 30 bars.

The results are in good agreement with the thermodynamic data according to the Le Chatelier law, indicate clearly that the highest CO_2 conversions as well as the highest DME selectivity could be obtained in the low temperatures range 200–220 °C [49]. It is desirable to have low CO selectivity, which results in a higher DME selectivity. In the rest of our work, the reaction temperature is fixed at 225 °C, in order to obtain the best selectivities towards CH_3OH and DME.

3.3 Effect of Mass Ratio

The effect of ZSM5-C/CZA weight ratio on the CO_2 hydrogenation reaction with different HZSM-5 loading (0.0–0.5 g) and a fixed CZA loading (0.125 g) disposed in dual-bed was investigated at 225 °C and 3 MPa.

By increasing the weight ratio of ZSM-5 to CZA from 0 to 0.8, the conversion of CO_2 passed through a maximum at 2.57% for ZSM5-C/CZA = 0.5. A higher ZSM5-C/CZA weight ratio was beneficial to the selectivity of DME, but a lower ZSM5-C/CZA ratio favoured the selectivity of CH_3OH (Table 4). The DME selectivity increased gradually with increasing the weight ration from 0 to 77%, but CH_3OH selectivity show the opposite response, which decreased from 100% for the pure catalyst CZA to 23.17% for the hybrid catalyst with the weight ratio of 0.8, which means that almost all of the CH_3OH formed is converted to DME.

The distribution of oxygenated products strongly depends on the ZSM5-C content of the hybrid catalyst. The selectivity to methanol decreases largely as ZSM5-C is added to the hybrid catalyst. These observations confirm that ZSM-5 is responsible for the formation of DME. The metal/acid ratio and the contact between both metal and acid catalysts are the key factors determining the efficiency of the catalyst for the direct production of DME from CO_2 [22, 50]. As shown in Table 4, the ZSM5-C/CZA weigh ratio equal to 0.33 leads to better CO_2 conversion with a high production of DME (382 g/h/kg_{cat}).

3.4 Influence of the Time on Steam

Figure 6 shows the conversion of carbone dioxide hydrogenation and product selectivities over CZA-ZSM5-C hybrid catalyst at 225 °C and 30 MPa as a function of time on stream (TOS). According to this figure, the equilibrium state is reached after a few minutes. As shown in Fig. 6, steady state conversion of CO_2 is maintained over 300 min of reaction. Product selectivities remain at steady state, affording 74% DME selectivity at 2.4% CO_2 conversion. Steady state methanol selectivity was 26% and the ratio of DME/CH_3OH was maintained throughout the 300 min testing period, indicating that the water vapor formed in CO_2 hydrogenation and methanol dehydration reactions is not affecting an online deactivation of the catalyst.

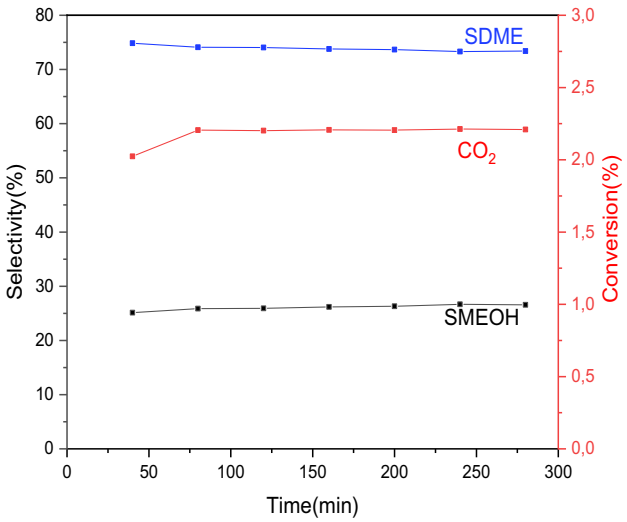

Fig. 6 CO_2 Conversions, CH_3OH and DME selectivities during a 5 h stability test of the CZA/ZSM5-C catalyst; reaction temperatures (225 °C)

It is evident that the catalyst was not subjected to deactivation, which means that carbon deposition did not occur, due to the absence of water gas shift reaction (RWGS) which favours the CO formation[51].

3.5 Catalytic Activity

The catalytic performance of hybrid catalysts with different size and shape, namely, CZA/ZSM5-C, CZA/ZSM5-P, CZA/ZSM5-H and CZA/ZSM5-HM were investigated in selective hydrogenation of carbon dioxide to dimethyl ether at 225 °C and P = 3.0 MPa. Under these conditions CO was not observed, only CH_3OH and DME as reaction products were obtained.

Table 4 Effects of mass ratio on the conversion of CO_2 and the product selectivity of CZA/ZSM5-C (p = 3.0 MPa, T = 225 °C, H_2/CO_2)

Weight ratio[a] CZA/ZSM5	Conversion CO_2 (%)	Selectivity (%)		Reaction rate (g/h/kg_{cat})		
		S_{CH3OH}	S_{DME}	CO_2	CH_3OH	DME
0.00	2.45	100.00	0.00	868	868	00
0.02	2.41	84.91	15.09	834	708	125
0.08	2.23	61.84	38.16	727	450	277
0.17	2.10	39.96	60.04	614	245	368
0.33	2.21	26.55	73.45	520	137	382
0.50	2.57	24.34	75.66	455	111	344
0.67	1.80	21.54	78.46	212	45	166
0.80	1.39	23.00	77.00	98	75	75

[a]The weight ratio is calculated by the equation: (masse of ZSM5/masse of CZA + masse of ZSM5)

Table 5 Effects of CO_2 Conversion and the product selectivity over different hybrid catalysts (P = 3.0 MPa, T = 225 °C, H_2/CO_2)

Samples	X_{CO_2}(%)	S_{CH3OH} (%)	S_{DME} (%)	Reaction rate (kg/h/kg_{cat})			Lewis acidity (μmol/g)	V_{meso} (m^3/g)
				CO_2	CH_3OH	DME		
CZA	2.4	100.0	–	0.86	0.86	–	–	–
CZA/ZSM5-C	2.2	26.5	73.5	0.52	0.14	0.38	36	0.10
CZA/ZSM5-P	2.9	24.3	75.6	0.68	0.16	0.51	36	0.18
CZA/ZSM5-H	2.3	27.7	72.3	0.54	0.15	0.39	29	0.17
CZA/ZSM5-HM	2.1	22.5	77.5	0.51	0.11	0.39	43	0.25

The reaction temperature, acidity and pore structure of zeolites can influence the catalytic performance in the conversion of CO_2 to CH_3OH and DME.

In our experiments, a good proportional correlation between the Lewis acidity and the DME selectivity is summarized in Table 5. As can be seen from the table, ZSM5-HM containing the highest Lewis acidity show the highest selectivity (77.5%). On the contrary, the lowest selectivity toward DME shown by ZSM5-H (72.3%) is in agreement with the lowest Lewis acidity of the catalyst. Meanwhile, CZA/ZSM5-C and CZA/ZSM5-P display moderate selectivity. The results are in good agreement with those Manuel Weber-Stockbauer et al. [52], have reported the stronger Lewis acid sites catalyze dimethyl ether formation via the Eley–Rideal mechanism in which methoxy groups react with gas phase methanol as the reactions below show:

$$CH_3OH_{(g)} + * \rightleftarrows CH_3 - O^* - H \quad (6)$$

$$CH_3 - O^* - H + CH_3OH_{(g)} \rightleftarrows CH_3OCH_{3(g)} + H - O^* - H \quad (7)$$

$$H - O^* - H \rightleftarrows H_2O_{(g)} + * ; \quad (* \text{ acid sites}) \quad (8)$$

However, the observed increase in the DME selectivity with the increase in the surface Lewis acid sites and mesopores volume strongly suggest that DME formation mainly occurs on Lewis acid sites, although the involvement of the Brønsted acid sites is also important [53, 54].

Previous works suggested [55, 56], that methanol conversion increased either by the scaling down of zeolite crystals to form a nanometer scale; or, by introducing mesopore into ZSM-5 crystals. Small and mesoporous ZSM-5 crystals with a higher external surface area offer more pore entrances than large crystals. This can explain why a higher selectivity of DME was achieved with the hollow mesoporous zeolite ZSM5-HM. The results clearly indicate that the products distributions over various hybrid catalysts are functions of external surface area, the nature acid sites and Si/Al ratio. Rownasghi et al. [57] examined both nano-ZSM-5 and mesoporous ZSM-5 zeolite

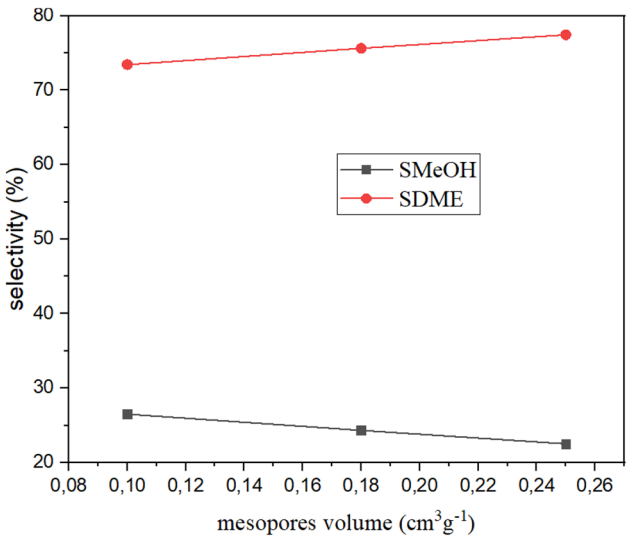

Fig. 7 Influence of mesopores volume on the selectivity of methanol and DME

at 225 °C in the methanol conversion to dimethyl ether. The best results were obtained using the nano-ZSM-5 zeolite with 100% selectivity of DME and 44% of CH_3OH conversion.

The correlation between selectivity to DME and the mesopores volume at 225 °C is plotted in Fig. 7. This graph showed that the selectivity to DME follows a linear increasing relationship with the mesopores volume, but the methanol selectivity showed the opposite response. We also found that the selectivity of DME over hybrid catalyst increased gradually with the decrease of Si/Al ratios from 34 to 28 (Table 1), although the amount of their acid sites increased.

The correlation between selectivity to methanol and DME and the amount of Lewis acid sites of the hybrid catalysts (see Table 1) relative to 225 °C is represented in Fig. 8. The results show good linear correlations between DME selectivity and Lewis acid content, but methanol selectivity is inversely proportional to the amount of Lewis acid sites.

The DME selectivity obtained over all the hybrid catalysts are compared in Fig. 9. It follows from this figure that

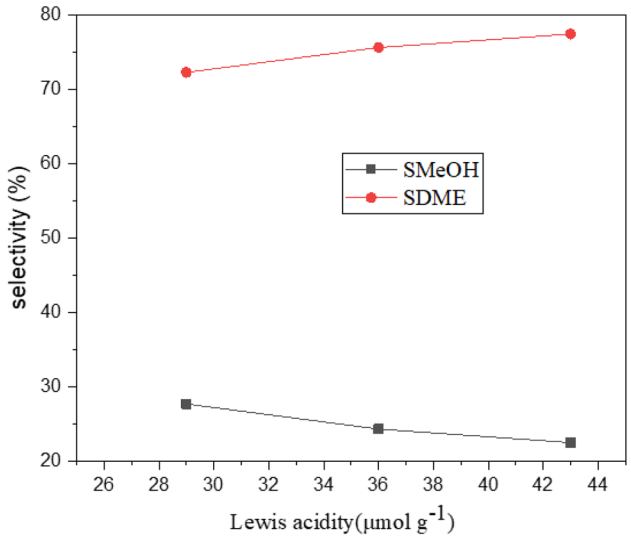

Fig. 8 Influence of acidity on the selectivity of methanol and DME

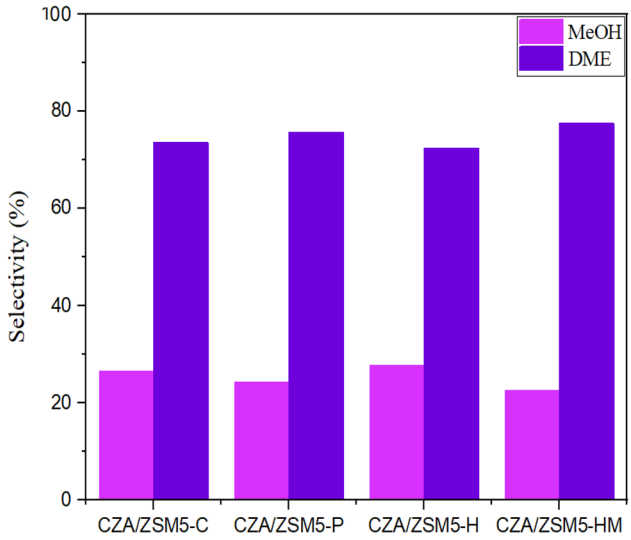

Fig. 9 Selectivity of methanol and DME over hybrid catalysts (T_R = 225 °C; P_R = 3.0 MPa; GHSV = 48,000 NL/h/kg_{cat})

DME selectivity of catalysts changed with the acidity of hybrid catalyst, mainly due to the change in methanol selectivity with the acid proprieties of hybrid catalysts. The CZA/ZSM5-HM gave higher selectivities of DME than CZA/ZSM5-P. Apparently, the high catalytic activity of CZA/ZSM5-HM was mainly due to their high accessibility of acid sites (when creating mesopores). The DME selectivity is basically proportional to mesopores volume and density of strong acid sites in catalyst. This result indicates that the acid site distribution determine the reaction selectivity, therefore, it is concluded that by reducing crystal size and also decreasing in the acid sites on the external surface are the certain ways to prove the selectivity to DME in carbon dioxide hydrogenation on CZA/ZSM5-HM hybrid catalyst. The low activity of CZA/ZSM5-P might be ascribed to the excessive decrease in the amount of acid sites, which showed the least value by both pyridine-IR and NH_3-TPD, although mesopores were also formed in its crystals during alkaline treatment. The presence of Lewis acid sites is a key parameter to promote the conversion of methanol to dimethyl ether. On all catalysts, the selectivity of dimethyl ether enhanced with the increase in Lewis acidity and mesopores volumes. The order of selectivity of DME is CZA/ZSM5-HM > CZA/ZSM5-P > CZA/ZSM5-H > CZA/ZSM5-C, which is the same order as external surface area.

4 Conclusion

A hollow nano-ZSM-HM zeolites with mesoporous shell was successfully synthesized by a two-step alkaline treatment method. Firstly, nano-ZSM-H zeolite was alkali treated with NaOH solution to dissolve internal silica of crystals and then the hollow structure was formed. After that, obvious mesopores were introduced in the shell of the hollow zeolites by a NaOH/TPAOH leaching based on the protective desilication. As a result, the external surface area was increased from 54 to 72 m^2/g, more than twice that of the untreated nano-ZSM-H. This hollow nano-ZSM-HM zeolite exhibited a large mesoporous volume of 0.25 m^3/g and a high Lewis acidity. The thin shell and rich mesopores would improve its catalytic performance in direct CO_2 hydrogenation to DME.

The hybrid catalyst (CZA/ZSM-HM) obtained from mesoporous hollow zeolite nano-ZSM-HM and Cu–ZnO/Al_2O_3 exhibits excellent DME selectivity (74%) and great stability throughout the reaction time. Higher concentration of Lewis acid zeolite and large mesopore volumes promote DME formation.

Declarations

Conflict of Interest The authors declare that they have no known competing financial interests or personal relationships that could have appeared to influence the work reported in this paper.

References

1. Brake LD (1986) Preparation of dimethylether by catalytic dehydration of methanol. U.S. Patent Documents. 4:595
2. van Dijk CP (1998) Dimtehyl ether production and recovery from methanol. U.S. Patent Documents. 5:750

3. Fleisch TH, Basu A, Sills RA (2012) Introduction and advancement of a new clean global fuel: The status of DME developments in China and beyond. J Nat Gas Sci Eng 9:94–107
4. Bradford MCJ, Konduru MV, Fuentes DX (2003) Preparation, characterization and application of Cr_2O_3/ZnO catalysts for methanol synthesis. Fuel Process technol. 83(1–3):11–25
5. Waugh K (1992) Methanol synthesis. Catal Today 15(1):51–75
6. Tidona B, Koppold C, Bansode A, Urakawa A, Von Rohr PR (2013) CO_2 hydrogenation to methanol at pressures up to 950bar. J Supercrit Fluids 78:70–77
7. Ruland H, Song H, Laudenschleger D, Stürmer S, Schmidt S, He J et al (2020) CO_2 Hydrogenation with Cu/ZnO/Al_2O_3: a Benchmark Study. Chem Cat Chem 12(12):3216–3222
8. Kim SM, Lee YJ, Bae JW, Potdar HS, Jun KW (2008) Synthesis and characterization of a highly active alumina catalyst for methanol dehydration to dimethyl ether. Appl Catal A Gen 348(1):113–120
9. Osman AI, Abu-Dahrieh JK, McLaren M, Laffir F, Nockemann P, Rooney D (2017) A facile green synthetic route for the preparation of highly active γAl_2O_3 from aluminum foil waste. Sci Rep 7:3593
10. Jiang S, Hwang JS, Jin T, Cai T, Cho W, Baek YS, Park SE (2004) Dehydration of methanol to dimethyl ether over ZSM-5 zeolite. Bull Korean Chem Soc 25(2):185–189
11. Ge Q, Huang Y, Qiu F, Li S (1998) Bifunctional catalysts for conversion of synthesis gas to dimethyl ether. Appl Catal A Gen 167(1):23–30
12. Brunetti A, Migliori M, Cozza D, Catizzone E, Giordano G, Barbieri G (2020) Methanol conversion to dimethyl ether in catalytic zeolite membrane reactors. ACS Sustain Chem Eng 8(28):10471–10479
13. Pérez-Fortes M, Schöneberger JC, Boulamanti A, Tzimas E (2016) Methanol synthesis using captured CO_2 as raw material: techno-economic and environmental assessment. Appl Energy 161:718–732
14. Alper E, Orhan OY (2017) CO_2 utilization: developments in conversion processes. Petroleum 3(1):109–126
15. Roy S, Cherevotan A, Peter SC (2018) Thermochemical CO_2 hydrogenation to single carbon products: scientific and technological challenges. ACS Energy Lett 3(8):1938–1966
16. Pérez-Fortes M, Tzimas E (2016) Techno-economic and environmental evaluation of CO_2 utilisation for fuel production: synthesis of methanol and formic acid.
17. Garcia-Trenco A, Martinez A (2012) Direct synthesis of DME from syngas on hybrid CuZnAl/ZSM-5 catalysts: new insights into the role of zeolite acidity. Appl Catal A Gen 411–412:170–179
18. Takeguchi T, Yanagisawa K, Inui T, Inoue M (2000) Effect of the property of solid acid upon syngas-to-dimethyl ether conversion on the hybrid catalysts composed of Cu-Zn-Ga and solid acids. Appl Catal A Gen. 192(2):201–209
19. Frusteri F, Cordaro M, Cannilla C, Bonura G (2015) Multifunctionality of Cu-ZnO-ZrO_2/H-ZSM5 catalysts for the one-step CO_2-to-DME hydrogenation reaction. Appl Catal B Envir 162:57–65
20. Bonura G, Frusteri F, Cannilla C, Ferrante GD, Aloise A, Catizzone E et al (2016) Catalytic features of CuZnZr-zeolite hybrid systems for the direct CO_2-to-DME hydrogenation reaction. Catal Today. 277:48–54
21. Aguayo AT, Erenã J, Sierra I, Olazar M, Bilbao J (2005) Deactivation and regeneration of hybrid catalysts in the single-step synthesis of dimethyl ether from syngas and CO_2. Catal Today 106(1–4):265–270
22. Li L, Mao D, Xiao J, Li L, Guo X, Yu J (2016) Facile preparation of highly efficient CuO-ZnO-ZrO_2/HZSM-5 bifunctional catalyst for one-step CO_2 hydrogenation to dimethyl ether: Influence of calcination temperature. Chem Eng Res and Des 111:100–108
23. Liu R, Qin Z, Ji H, Su T (2013) Synthesis of dimethyl ether from CO_2 and H_2 using a Cu-Fe-Zr/HZSM-5 catalyst system. Ind Eng Chem Res 52(47):16648–16655
24. Fang X, Jia H, Zhang B, Li Y, Wang Y, Song Y et al (2021) A novel in situ grown Cu-ZnO-ZrO_2/HZSM-5 hybrid catalyst for CO_2 hydrogenation to liquid fuels of methanol and DME. J Environ Chem Eng. 9(4):105299
25. Zhou X, Su T, Jiang Y, Qin Z, Ji H, Guo Z (2016) CuO-Fe_2O_3-CeO_2/HZSM-5 bifunctional catalyst hydrogenated CO_2 for enhanced dimethyl ether synthesis. Chem Eng Sci 153:10–20
26. Qin ZZ, Zhou XH, Su TM, Jiang YX, Ji HB (2016) Hydrogenation of CO_2 to dimethyl ether on La-, Ce-modified Cu-Fe/HZSM-5 catalysts. Catal Commun 75:78–82
27. Fu T, Qi R, Wang X, Wan W, Li Z (2017) Facile synthesis of nano-sized hollow ZSM-5 zeolites with rich mesopores in shell. Micr Meso Mater 250:43–46
28. Mao D, Yang W, Xia J, Zhang B, Song Q, Chen Q (2005) Highly effective hybrid catalyst for the direct synthesis of dimethyl ether from syngas with magnesium oxide-modified HZSM-5 as a dehydration component. J Catal 230(1):140–149
29. Khandan N, Kazemeini M, Aghaziarati M (2008) Determining an optimum catalyst for liquid-phase dehydration of methanol to dimethyl ether. Appl Catal A Gen 349(1–2):6–12
30. Ateka A, Pérez-Uriarte P, Sierra I, Ereña J, Bilbao J, Aguayo AT (2016) Regenerability of the CuO-ZnO-MnO/SAPO-18 catalyst used in the synthesis of dimethyl ether in a single step. Reac Kinet Mech Cat 119:655–670
31. Şeker B, Dizaji AK, Balci V, Uzun A (2021) MCM-41-supported tungstophosphoric acid as an acid function for dimethyl ether synthesis from CO_2 hydrogenation. Ren Ener 171:47–57
32. Frusteri F, Bonura G, Cannilla C, Ferrante GD, Aloise A, Catizzone E et al (2015) Stepwise tuning of metal-oxide and acid sites of CuZnZr-MFI hybrid catalysts for the direct DME synthesis by CO_2 hydrogenation. Appl Catal B Environ 176–177:522–531
33. Kornas A, Śliwa M, Ruggiero-Mikołajczyk M, Samson K, Podobiński J, Karcz R et al (2020) Direct hydrogenation of CO_2 to dimethyl ether (DME) over hybrid catalysts containing CuO/ZrO_2 as a metallic function and heteropolyacids as an acidic function. Reac Kinet Mech Cat 130:179–194
34. Xu M, Lunsford JH, Goodman DW, Bhattacharyya A (1997) Synthesis of dimethyl ether (DME) from methanol over solid-acid catalysts. Appl Catal A Gen 149(2):289–301
35. Vishwanathan V, Jun KW, Kim JW, Roh HS (2004) Vapour phase dehydration of crude methanol to dimethyl ether over Na-modified H-ZSM-5 catalysts. Appl Catal A Gen 276(1–2):251–255
36. Ahouari H, Soualah A, Le Valant A, Pinard L, Pouilloux Y (2015) Hydrogenation of CO_2 into hydrocarbons over bifunctional system Cu–ZnO/Al_2O_3 + HZSM-5: effect of proximity between the acidic and methanol synthesis sites. C R Chimie 18(12):1264–1269
37. Bonnin A, Comparot JD, Pouilloux Y, Coupard V, Uzio D, Pinard L (2021) Mechanisms of aromatization of dilute ethylene on HZSM-5 and on Zn/ HZSM-5 catalysts. Appl Catal A Gen. 611:117971
38. Tao Y, Kanoh H, Kaneko K (2003) ZSM-5 monolith of uniform mesoporous channels. J Am Chem Soc 125(20):6044–6045
39. Batonneau-Gener I, Sachse A (2019) Determination of the exact microporous volume and BET surface area in hierarchical ZSM-5. J Phys Chem C. 123(7):4235–4242
40. Hardenberg TAJ, Mertens L, Mesman P, Muller HC, Nicolaides CP (1992) A catalytic method for the quantitative-evaluation of crystallinites of ZSM-5 zeolite preparations. Zeolites 12(6):685–689
41. Karge HG (1991) Comparative measurements on acidity of zeolites. Stud Surf Sci Catal 65:133–156

42. Datka J, Gil B, Baran P (2003) Heterogeneity of OH groups in HZSM-5 zeolites: splitting of OH and OD bands in low-temperature IR spectra. Micr Meso Mater 58(3):291–294
43. Rosenberg DJ, Anderson JA (2004) On the environment of the active sites in phosphate modified silica-zirconia acid catalysts. Catal Lett 94:109–113
44. Sadowska K, Góra-Marek K, Datka J (2012) Hierarchic zeolites studied by IR spectroscopy: acid properties of zeolite ZSM-5 desilicated with NaOH and NaOH/tetrabutylamine hydroxide. Vib Spectrosc 63:418–425
45. Bonura G, Cordaro M, Cannilla C, Mezzapica A, Spadaro L, Arena F, Frusteri F (2014) Catalytic behaviour of a bifunctional system for the one step synthesis of DME by CO_2 hydrogenation. Catal Today 228:51–57
46. Rodriguez-Gonzalez L, Hermes F, Bertmer M, Rodriguez-Castellon E, Jimenez-Lopez A, Simon U (2007) The acid properties of H-ZSM-5 as studied by NH_3-TPD and 27Al-MAS-NMR spectroscopy. Appl Catal A 328(2):174–182
47. Frusteri F, Migliori M, Cannilla C, Frusteri L, Catizzone E, Aloise A et al (2017) Direct CO_2-to-DME hydrogenation reaction: New evidences of a superior behaviour of FER-based hybrid systems to obtain high DME yield. J of CO2 Utilization. 18:353–361
48. Ordomsky VV, Cai M, Sushkevich V, Moldovan S, Ersen O, Lancelot C et al (2014) The role of external acid sites of ZSM-5 in deactivation of hybrid CuZnAl/ZSM-5 catalyst for direct dimethyl ether synthesis from syngas. Appl Catal A Gen 486:266–275
49. Huang MH, Lee HM, Liang KC, Tzeng CC, Chen WH (2015) An experimental study on single-step dimethylether (DME) synthesis from hydrogen and carbon monoxide under various catalysts. Int J Hydr Ener 40:13583–13593
50. Catizzone E, Bonura G, Migliori M, Braccio G, Frusteri F, Giordano G (2019) Direct CO_2 -to-dimethyl ether hydrogenation over CuZnZr/zeolite hybrid catalyst: new evidence on the interaction between acid and metal sites. Ann Chim Sci Mat 43:141–149
51. Ereña J, Sierra I, Olazar M, Gayubo AG, Aguayo AT (2008) Deactivation of a CuO-ZnO-Al_2O_3/γ-Al_2O_3 catalyst in the synthesis of dimethyl ether. Ind Eng Chem Res 47(7):2238–2247
52. Weber-Stockbauer M, Gutiérrez OY, Bermejo-Deval R, Lercher JA (2019) The role of weak Lewis acid sites for methanol thiolatio. Catal Sci Tech. 9:255–520
53. Akarmazyan SS, Panagiotopoulou P, Kambolis A, Papadopoulou C, Kondarides DI (2014) Methanol dehydration to dimethyl ether over Al_2O_3 catalysts. Appl Catal B Environ 145:136–148
54. Osman AI, Abu-Dahrieh JK, Rooney DW, Thompson J, Halawy SA, Mohamed MA (2017) Surface hydrophobicity and acidity effect on alumina catalyst in catalytic methanol dehydration reaction. J Chem Technol Biotechnol 92(12):2952–2962
55. Fu T, Wang Y, Li Z (2010) Surface-Protection-Induced controllable restructuring of pores and acid sites of the nano-zsm-5 catalyst and its influence on the catalytic conversion of methanol to hydrocarbons. Langmuir 36(14):3737–3749
56. Yu DK, Fu ML, Yuan YH, Song YB, Chen JY, Fang YW (2016) One-step synthesis of hierarchical-structured ZSM-5 zeolite. J Fuel Chem Technol 44(11):1363–1369
57. Rownaghi AA, Rezaei F, Stante M, Hedlund J (2012) Selective dehydration of methanol to dimethyl ether on ZSM-5 nanocrystals. Appl Catal B Environ 119–120:56–61